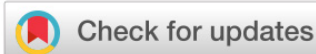


Original Research

View Article online



Received 14 March 2025

Revised 12 May 2025

Accepted 12 May 2025

Available Online 03 July 2025

Edited by Kannan RR Rengasamy

KEYWORDS:

Durian
Sun screen protection
Nitric oxide suppression
Antioxidant
Cytotoxicity

Natr Resour Human Health 2025; 5 (3): 449–461
<https://doi.org/10.53365/nrhh/204985>
eISSN: 2583-1194
Copyright © 2025 Visagaa Publishing House

Photoprotective Property, Bioactivities, and Chemical Composition of Durian Peel Extracts: Agricultural Waste Valorization for Cosmetic and Pharmaceutical Applications

Awat Wisetsai^{1*}, Lueacha Tabtimmai^{2,3}, Chanikan Sonklin¹, Anupong Joompang⁴, Nuttakarn Srisukpachin¹, Supachai Jadsadajerm¹, Sutarin Preepram¹

¹Industrial Chemistry, Faculty of Applied Science, King Mongkut's University of Technology North Bangkok, Thailand

²Biotechnology, Faculty of Applied Science, King Mongkut's University of Technology North Bangkok, Thailand

³Food and Agro-Industrial Research Center, King Mongkut's University of Technology North Bangkok, Thailand

⁴Division of Pharmacology and Biopharmaceutical Sciences, Faculty of Pharmaceutical Sciences, Burapha University, Thailand

ABSTRACT: This study explores the bioactive properties of Thai *Durio zibethinus* (Montong durian) peel extracts, focusing on their potential for therapeutic applications in the nutraceutical and cosmetic industries. The extracts were evaluated for their cytotoxic, antioxidant, anti-inflammatory, and photoprotective activities. The *n*-hexane extract demonstrated potent cytotoxic effects against HCT116 colorectal cancer cells, achieving 98.23% inhibition at 50 µg/mL, with an IC₅₀ value of 43.04 ± 4.64 µg/mL. The EtOAc extract displayed significant anti-inflammatory effects, inhibiting nitric oxide production in LPS-stimulated RAW 264.7 macrophage cells, with an IC₅₀ of 6.02 ± 0.65 µg/mL. Antioxidant activity, measured through DPPH and ABTS assays, was the highest in the EtOAc extract. The photoprotective potential was confirmed through SPF evaluation, indicating UV protection across tested concentrations. GC/MS analysis of the *n*-hexane extract identified key bioactive constituents, including phytosterols. Guided by bioactivity results, 10 compounds were isolated from the *n*-hexane and EtOAc extracts, with compounds 3, 4, and 5 identified for the first time from the *Durio* genus. Structural elucidation using 1D and 2D NMR spectroscopy confirmed the identities of these compounds. These findings highlight the promising applications of *D. zibethinus* peel extracts as sources of bioactive compounds for health-related industries.

1. INTRODUCTION

Durian (*Durio zibethinus* Murr.) is widely regarded as one of the most popular and sought-after fruits in Thailand and

Southeast Asia. It is valued for its rich nutritional content and distinctive flavor (He et al., 2023). In 2019, the area under durian cultivation in Malaysia was 72,536 hectares, yielding an output of 384,170 tons. In 2020, production of durian was

* Corresponding author.

E-mail address: awat.w@sci.kmutnb.ac.th (Awat Wisetsai)

This is an open access article under the CC BY-NC-ND license (<http://creativecommons.org/licenses/by-nc-nd/4.0/>).

1.2 million tons in Indonesia and 110,000 tons in Thailand (Zhan et al., 2021). However, consumption of durian generates substantial waste, as the peels, seeds, and other inedible parts constitute 40–55% of the entire fruit (Pimsamarn et al., 2024). The outer shell alone accounts for over half of the durian's total weight, leaving only 15–30% as the edible portion. Consequently, about 70–85% of the fruit is discarded as waste, leading to environmental concerns if not properly handled (Payus et al., 2021).

Current research on durian primarily emphasizes the preservation of its pulp and various processing techniques (Phoengmak et al., 2023; Tan et al., 2020). Regarding waste management, existing studies have investigated the potential of using durian peel waste for energy production (Numeet et al., 2024; Pimsamarn et al., 2024). However, research on developing medicinal products from durian shells is limited, leading to an underutilization of potentially valuable medicinal resources. This issue is particularly notable in Thailand, one of the largest producers of durian peel waste, where various parts of the durian tree including the leaves, bark, pulp, seeds, and peel are recognized for their nutritional benefits and applications in traditional medicine across Southeast Asia. Specifically, durian leaves are utilized in the preparation of medicinal baths for the treatment of jaundice, while the pulp is known for its anti-helminthic effects. In addition, ash from burned durian peel is traditionally ingested following childbirth, and the bark sap is employed as a treatment for malaria (Charoenphun and Klangbud, 2022; Zhan et al., 2021).

Previous phytochemical investigations of durian fruits have facilitated the isolation and identification of secondary metabolites such as flavonoids, fatty acids, sulfur-containing compounds, and polysaccharides (Charoenkiatkul et al., 2016; Cuong et al., 2023; Feng et al., 2016; Feng et al., 2018; Kongkachuichai et al., 2010). Durian peel has shown potential for antioxidant, anti-inflammatory, and anticancer properties. Feng and colleagues reported that durian peel from China contains triterpenoids and glycosides with anti-inflammatory effects, specifically inhibiting lipopolysaccharide (LPS)-induced nitric oxide (NO) production in the RAW 264.7 cell line (Feng et al., 2018). In contrast, it has been noted that only the inner peel of durian harvested in Thailand demonstrates anti-NO and antioxidant activities (Charoenphun and Klangbud, 2022). However, the specific bioactive compounds responsible for these effects remain unidentified. Moreover, fruit peel extracts from durian cultivated in Hanoi, Vietnam, have demonstrated cytotoxic activity against MCF7, HepG2, and SK-LU-1 cancer cell lines (Cuong et al., 2023). To date, comparable cytotoxic properties have not been documented for durian peel waste originating from Thailand, highlighting a gap in investigating its potential bioactive constituents.

Given these findings, identifying and purifying the active compounds responsible for the anticancer, anti-inflammatory, and antioxidant properties of agricultural waste products in Thailand is essential for evaluating their potential in cosmetic and pharmaceutical applications. This study focuses on assessing the anti-inflammatory, anticancer (HCT116 cell line), antioxidant, and photoprotective activities of extracts, aiming to isolate and identify the active compounds responsible for these effects. The results are expected to support waste reduction efforts by converting durian peel into valuable nutraceuticals and exploring potential applications in functional foods, cosmetics, and pharmaceuticals for enhanced health benefits.

2. MATERIALS AND METHODS

2.1. General experimental procedures

NMR spectra were acquired on a Bruker Avance 400 NMR spectrometer (Bruker, Germany) using CDCl_3 and CD_3OD as solvents. Chemical shifts were recorded in δ (ppm) using the solvent's residual peak (^1H NMR) or the solvent's peak (^{13}C NMR) as internal standards. Column chromatography (CC) was carried out on MERCK silica gel 60 (230–400 mesh) (Merck, Darmstadt, Germany), and Sephadex LH-20 was used for CC. Thin-layer chromatography (TLC) was carried out with pre-coated MERCK silica gel 60 PF254 (Merck, Darmstadt, Germany); the spots were visualized under UV light (254 and 365 nm) and further stained by spraying *p*-anisaldehyde and then heated until charred. Unless otherwise noted, all chemicals were obtained from commercially available sources and were used without further purification.

2.2. Plant material

Durian peels were obtained from Montong durian fruits (*D. zibethinus*) cultivated in the Rayong Province, Thailand. The preparatory procedures prior to use were conducted in accordance with the methodologies outlined in our previous publication (Pimsamarn et al., 2024).

2.3. Chemical analysis

2.3.1. Determination of total phenols

Total polyphenol content was quantified spectrophotometrically via the Folin–Ciocalteu method, measuring absorbance at 765 nm. Gallic acid was used as the calibration

standard, and results were expressed in milligrams of gallic acid equivalents (mg GAE) per gram of dry weight (DW), as described by the previous report (Arancibia-Avila et al., 2008).

2.3.2. GC/MS analysis

The GC/MS analysis was conducted employing an Agilent 7697A GC/MS system, which was connected to an Agilent 7890B (Agilent Technologies Inc, Santa Clara, CA). For the separation of chemical components, the HP5 column (30 m × 0.25 mm, 0.25 mm film thickness) was utilized, and helium (purity 99.99%) served as the carrier gas at a flow rate of 1.2 mL/min. The GC oven temperature was initially set at 70°C for 10 minutes, followed by a gradual increase to 300°C at a rate of 5°C/minutes, and then held constant at 300°C for an additional 10 minutes. A split ratio of 20:1 was employed. The injector temperature was adjusted to 250°C, and mass spectra were acquired with the MS quad temperature set at 150°C and the MS source temperature at 230°C. The mass range for the analysis was configured from 20 to 400 m/z. The chemical compositions were identified by comparing their mass spectra with those from the NIST Mass Spectra Library (NIST 08 Mass Spectra Library, Version 2.0 f). The relative amounts of individual components were calculated based on the GC peak area (FID response) without applying a correction factor.

2.3.3. Extraction and isolation

The air-dried powdered peels of Monthong durian (3.0 kg) were extracted with MeOH (each, 3 × 10 L) by maceration in a solvent at room temperature for 3 days. Removal of the solvent under reduced pressure gave the crude MeOH (175.0 g). The crude MeOH was suspended in water (1 L) and then sequentially extracted with *n*-hexane (1 L), EtOAc (1 L), and *n*-butanol (1 L) to afford *n*-hexane extract (52.0 g, 1.73 % w/w dry powder), EtOAc extract (45.0 g, 1.5 % w/w dry powder), and finally *n*-butanol extract (68.0 g, 2.27 % w/w dry powder).

Thirteen grams of the *n*-hexane extract was further fractionated by silica gel CC using an *n*-hexane gradient with increasing polarity. Each fraction (150 mL) was monitored by TLC, and those with similar TLC profiles were combined to yield five main fractions labeled DH1–DH5. Fraction DH4 was purified by silica gel CC using an isocratic system of *n*-hexane (8:2), resulting in a mixture of compounds **8** and **9** (5.0 g) as white amorphous powders.

Forty grams of the crude EtOAc extract was fractionated on silica gel using a gradient system of *n*-hexane followed by EtOAc, with increasing polarity, to yield six fractions (DE1–DE6). Fraction DE3 was further fractionated on Sephadex LH-20 using 100% MeOH, resulting in three subfractions

(DE3.1–DE3.3). Subfraction DE3.3 was subsequently purified by silica gel CC with an isocratic elution of CH₂Cl₂ (9:1), yielding compounds **6** (20.0 mg) and **7** (9.0 mg) as white amorphous solids. Fraction DE4 was subjected to silica gel CC, following a similar gradient system as that used for the crude EtOAc extract, making four subfractions (DE4.1–DE4.4). Subfraction DE4.4 was further purified by silica gel CC with an isocratic elution of *n*-hexane:EtOAc (7:3), yielding compounds **1** (10.2 mg), **2** (8.5 mg), and **3** (15.2 mg) as white amorphous solids. Compounds **4** (4.5 mg) and **5** (7.6 mg) were isolated as white amorphous solids by further purification with Sephadex LH-20 using 100% MeOH. Fraction DE6 was washed with EtOAc to afford compound **10** (30.2 mg) as a white amorphous solid.

2.4. Biological activities

2.4.1. Cell culture and cytotoxicity assay

HCT116 and *Vero* (CCL-81) cells were purchased from the American Type Culture Collection. The cells were routinely grown in Dulbecco's Modified Eagle Medium (DMEM) (Gibco) supplemented with 10% FBS (Cytiva) and 1% penicillin-streptomycin solution (Gibco) at 37°C, 5% CO₂ in a humidified atmosphere in an incubator. The cells were passaged every 3 days. The cytotoxic activity of samples was evaluated by MTT assay. HCT116 (7 × 10³) and *Vero* (2 × 10³) cells were plated into a 96-well plate. After 16–18 h, the attached cells were replenished with a fresh culture medium containing various concentrations of each sample and incubated for another 72 h. At that time, the treated cells were replaced with fresh culture medium supplemented with 0.5 mg/mL MTT solution. After 3 h of incubation, the medium was discarded, and the formed purple formazan crystals were completely dissolved by adding 50 µL of DMSO. Absorbance was measured at 570 and 630 nm as a measurement and reference wavelength, respectively. To generate a nonlinear regression curve, a dose-dependent experiment was conducted over a concentration range of 4.69–300 µg/mL for *Vero* cells and 6.25–200 µg/mL for HCT116 colorectal cancer cells. The IC₅₀ value was determined using the Prism11 software. Doxorubicin was used as a positive control drug.

2.4.2. NO inhibition and cell viability assays

2.4.2.1. Cell culture

RAW 264.7 cells were cultured in RPMI supplemented with 10% heat-inactivated FBS, 1% penicillin–streptomycin solution, and 5% L-glutamine under 37°C, 5% CO₂, and 90% relative humidity incubator (Tabtimmai et al., 2024).

2.4.2.2. Cell viability assay

The assays were carried out in triplicate using the same approach as in the prior publication with minor modifications (Tabtimmai et al., 2024). Briefly, Raw 264 cells (10,000 cell/well) were seeded in a 96-well plate overnight. Then, the cells were treated with different concentrations (4.69–300 µg/mL) of sample for 24 h. After that, the medium was removed and the cells were incubated with 150 µL of 3-(4,5-dimethylthiazol-2-yl)-2,5-diphenyl-2H-tetrazolium bromide (MTT) (0.5 mg/mL) for 4 hours. The formazan crystal was dissolved with DMSO and the absorbance at 570 nm was detected using spectrophotometer. The percentage of cell viability was calculated as compared to the absorbance of treated cells with untreated cells.

2.4.2.3. NO production assay

The assays were carried out in triplicate using the same approach as in the prior publication with minor modifications (Tabtimmai et al., 2024). Briefly, Raw 264 cells (10,000 cells/well) were seeded in a 96-well plate overnight. The treated cells were stimulated by adding 1 µg/mL LPS for another 24 hours. Then, the cells were treated with 150 µL of difference concentrations (4.69–300 µg/mL) of extract samples for 24 hours. For pure compounds (1–7), the concentration of 75 µM was used to screen the NO suppression. LPS-stimulated cells were used as a positive control. At the time, the conditioned medium was collected to determine released NO using Griess's reagent. The amount of released NO was calculated regarding the NO calibration curve. The remaining cells were assessed for cell viability using the MTT method as described above.

2.5. Determination of free radical scavenging activity

2.5.1. 1,1-Diphenyl-2-picrylhydrazyl radical (DPPH•) scavenging activity

The DPPH radical scavenging activity of the samples was evaluated following the method described in previous studies, with trolox used as the standard (Sonklin et al., 2021). The percentage of DPPH radical scavenging activity was calculated using Equation (1):

$$\text{DPPH radical scavenging activity (\%)} = \frac{A_b - A_s}{A_b} \times 100 \quad (1)$$

where A_b is the absorbance of the blank, and A_s is the absorbance of the sample.

2.5.2. Hydroxyl radical scavenging activity

The hydroxyl radical scavenging efficacy of each sample was assessed as previously described, with trolox used as the

standard (Sonklin et al., 2021). The scavenging potency was expressed as the percentage inhibition (%) calculated using Equation (2):

$$\text{Hydroxyl radical scavenging activity \%} = \frac{\Delta A \text{ min}^{-1}(\text{blank}) - \Delta A \text{ min}^{-1}(\text{sample})}{\Delta A \text{ min}^{-1}(\text{blank})} \times 100 \quad (2)$$

2.5.3. Superoxide anion radical scavenging activity

The superoxide anion radical scavenging efficacy of each sample was determined according to previously established protocols, using trolox as the standard (Sonklin et al., 2021). The percentage inhibition of scavenging activity was calculated using Equation (3):

$$\text{Superoxide radical scavenging activity \%} = \frac{\Delta A \text{ min}^{-1}(\text{blank}) - \Delta A \text{ min}^{-1}(\text{sample})}{\Delta A \text{ min}^{-1}(\text{blank})} \times 100 \quad (3)$$

2.5.4. Hydrogen peroxide radical scavenging activity

The hydrogen peroxide radical scavenging efficacy of different solvent extracts was measured following previously reported methodologies (Sonklin et al., 2021). The scavenging activity was expressed as the percentage inhibition according to Equation (4):

$$\text{Hydroxyl radical scavenging activity \%} = \frac{\Delta A \text{ min}^{-1}(\text{blank}) - \Delta A \text{ min}^{-1}(\text{sample})}{\Delta A \text{ min}^{-1}(\text{blank})} \times 100 \quad (4)$$

2.5.5. Ferric reducing antioxidant power (FRAP)

The FRAP assay was performed according to a modified method, as described by Karamać et al. (2016). A standard curve was generated using $\text{FeSO}_4 \cdot 7\text{H}_2\text{O}$ (0.03–0.9 µmol/mL). The absorbance of each sample was converted to mmol Fe^{2+} reduced per gram of sample, based on the regression slope of the standard curve.

2.6. SPF in vitro of the crude extracts

The photoprotective potential of *D. zibethinus* peel extracts was assessed using the method described by Mota et al. (2020) with modifications. Crude extract solutions were prepared at final concentrations of 100, 500, and 1000 ppm. Absorbance measurements for each concentration were conducted in triplicate using a VICTOR® Nivo™ Multimode Plate Reader (PerkinElmer), within the UV spectrum range of 290–320 nm at 5 nm increments, with ethanol as

the blank. SPF values were then determined according to Equation (5).

$$\text{SPF} = \text{CF} \cdot \sum_{290}^{320} \text{EE}(\lambda) I(\lambda) \text{Abs}(\lambda) \quad (5)$$

where *CF* is the correction factor, set to 10; the erythral effect spectrum, denoted as *EE*(λ); the solar intensity spectrum, represented by *I*(λ); and *Abs*(λ), the absorbance of the extract at each wavelength (λ). The values of *EE* \times *I* are constant values (Albuquerque *Nerys et al.*, 2022).

2.7. Molecular docking

The interaction between compounds **1** and **2** and the TLR4/MD2 receptor complex was predicted using GOLD

Suite 5.5 (Cambridge Crystallographic Data Center, Cambridge, UK) (Figure 1). The crystal structure of the TLR4/MD2/neoseptin-3 receptor complex (PDB ID: 5ijc) was prepared by removing water molecules and ligands using Discovery Studio 2017 R2 Client (Dassault Systèmes BIOVIA, BIOVIA Workbook, Release 2017; BIOVIA Pipeline Pilot, Release 2017; San Diego: Dassault Systèmes). The structures of **1** and **2** were drawn in ChemDraw (ChemDraw Professional 17.1) and subsequently subjected to energy minimization using HyperChem 8.0 (HyperChem, Release 8.0 for Windows, Molecular Modeling System: HyperCube, 2007). Flexible docking of compounds **1** and **2** was performed within the TLR4/MD2 receptor complex (Chains B and C) at the neoseptin-3 binding site, using a 6 Å radius. The GOLD docking procedure was executed with 10 GA runs and a search efficiency of 200%, while all other parameters were set to default. Docking accuracy was

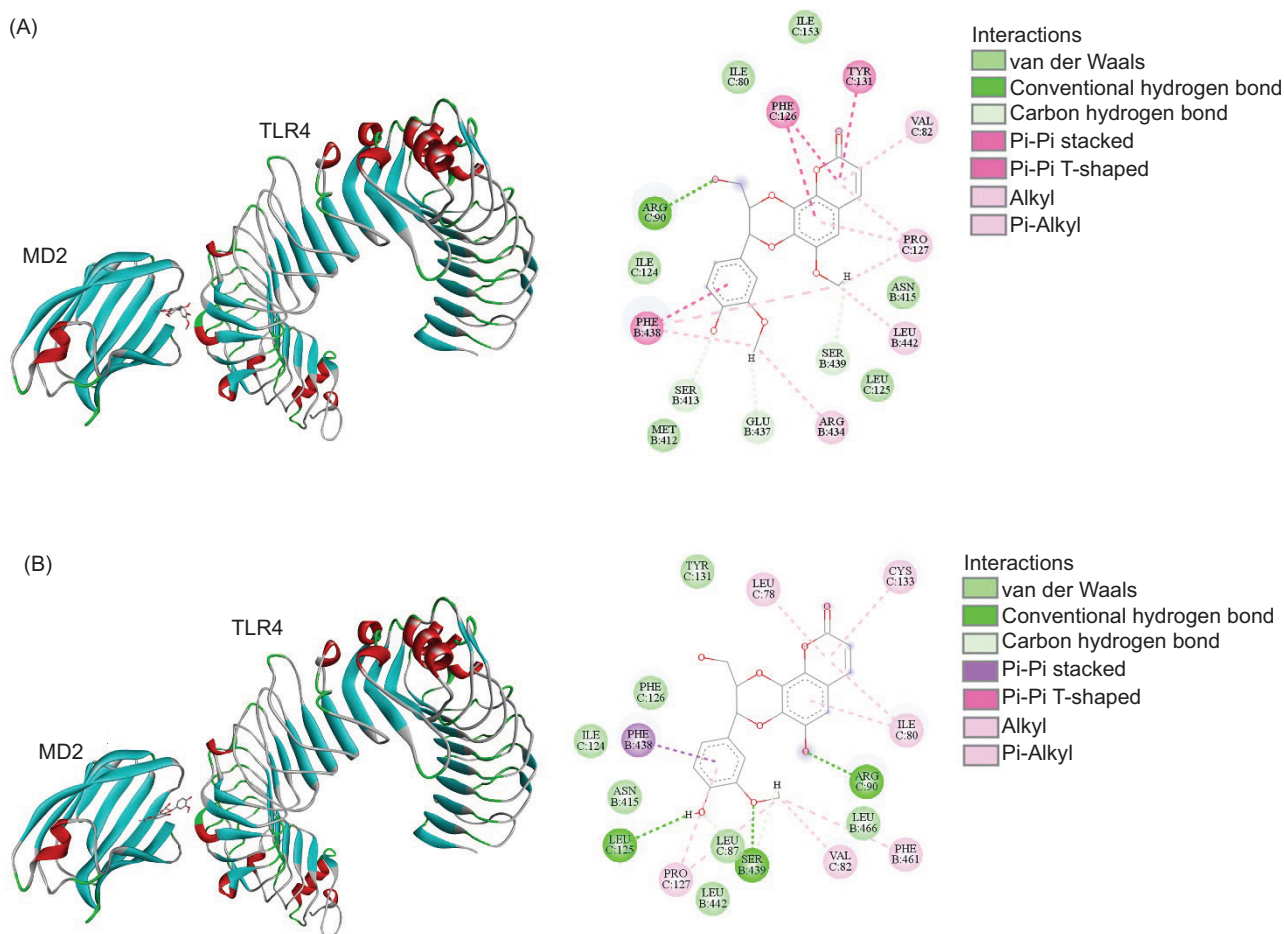


Figure 1. Interaction of compounds **1** (A) and **2** (B) with the TLR4/MD2 receptor complex. The images were created and modified using Discovery Studio 2017 R2 Client. In the figures, amino acids from the MD2 subunit are labeled as C, while those from the TLR4 subunit are labelled as B.

validated by self-docking of neoseptin-3 into its binding site, yielding an RMSD of less than 2 Å. The **1** or **2** complexes with the highest GOLD fitness score was selected for representation. The types of interactions were analyzed using Discovery Studio 2017 R2 Client.

3. RESULTS

3.1. Cytotoxic activity evaluation of *D. zibethinus* crude extracts

The cytotoxic potential of *D. zibethinus* peel extracts against HCT116 colorectal cancer cells was evaluated using the MTT assay. Among the extracts tested, the *n*-hexane extract demonstrated notable cytotoxicity, with an inhibition rate of 98.23% at 50 µg/mL, significantly surpassing the inhibitory effects of the ethyl acetate (EtOAc) and *n*-butanol extracts, which exhibited inhibition rates below 50% at the same concentration. The IC₅₀ for the *n*-hexane extract was determined as 43.04 ± 4.64 µg/mL (Table 1). These findings highlight the superior inhibitory efficacy of the *n*-hexane extract on HCT116 cells relative to EtOAc and *n*-butanol extracts. To identify the bioactive constituents contributing to this cytotoxicity, gas chromatography-mass spectrometry (GC-MS) analysis and chromatographic methods were employed to elucidate the metabolite profile of the *n*-hexane extract.

3.2. Evaluation of antioxidant activities of *D. zibethinus* crude extracts

The antioxidant activities of the *D. zibethinus* peel extracts (*n*-hexane, EtOAc, and *n*-butanol) were initially assessed through IC₅₀ values in DPPH and ABTS radical scavenging assays to guide further antioxidant evaluation. The *n*-hexane extract demonstrated no notable antioxidant activity (>2 mg/mL) in both assays (Table 2). In contrast, the EtOAc

extract exhibited strong antioxidant potential, with IC₅₀ values of 0.109 ± 0.01 mg/mL and 0.051 ± 0.002 mg/mL in the DPPH and ABTS assays, respectively. The *n*-butanol extract showed moderate antioxidant activity, achieving IC₅₀ values of 0.199 ± 0.002 mg/mL and 0.077 ± 0.006 mg/mL in the DPPH and ABTS assays, respectively. Subsequently, the EtOAc and *n*-butanol extracts, as the most active extracts, were further evaluated using hydroxyl radical (•OH), superoxide anion (O₂•⁻), and FRAP assays. The results confirmed a similar trend, with EtOAc consistently exhibiting potent activity across assays, while the *n*-butanol extract showed inactivity in the O₂•⁻ assay. The EtOAc and *n*-butanol extracts achieved FRAP values of 0.053 ± 0.003 and 0.034 ± 0.01 mM Fe²⁺/mg, respectively. Collectively, these findings underscore the fact that the EtOAc extract is the most effective antioxidant among those tested.

3.3. Anti-inflammatory property evaluation of *D. zibethinus* crude extracts

The anti-inflammatory properties of the three crude extracts from *D. zibethinus* peels were evaluated through NO

Table 1

Cytotoxicity of extracts in HCT116 colorectal cancer and *Vero* cells by MTT assays.

Crude extracts	IC ₅₀ (µg/mL)	
	HCT116	<i>Vero</i>
<i>n</i> -hexane	43.04 ± 4.64	160.89 ± 2.53
EtOAc	ND	184.64 ± 10.00
<i>n</i> -butanol	ND	182.38 ± 3.27

ND = not determined.

In = inactive.

Table 2

Antioxidant activities of *n*-hexane, EtOAc, and *n*-butanol extracts of *D. zibethinus* peels.

Samples	IC ₅₀ (mg/mL)				FRAP
	DPPH	ABTS	•OH	O ₂ • ⁻	mM Fe ²⁺ /mg
<i>n</i> -hexane	In	In	In	In	In
EtOAc	0.109 ± 0.01	0.051 ± 0.002	0.329 ± 0.09	0.188 ± 0.07	0.053 ± 0.003
<i>n</i> -butanol	0.199 ± 0.002	0.077 ± 0.006	1.40 ± 0.11	In	0.034 ± 0.01
Trolox*	0.003 ± 0.0001	0.006 ± 0.0001	88.79 ± 2.37%**	0.3486 ± 0.039	0.668 ± 0.07

In = inactive (IC₅₀ > 2 mg/mL).

*Positive control (mM).

**Activity value was determined at 0.1 mg/mL of trolox.

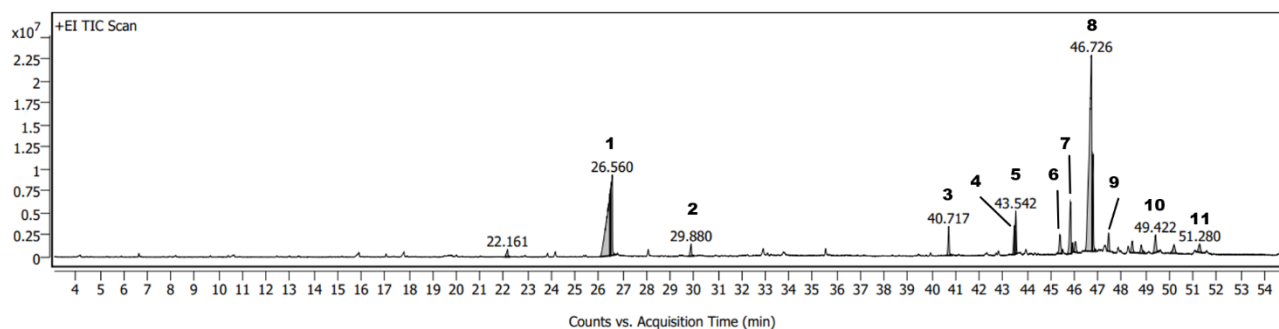


Figure 2. Total ion chromatogram of the *n*-hexane extract of *D. zibethinus* peels. Compound peaks were ranked by number.

suppression activity, measured by their IC_{50} values for inhibiting NO production in LPS-activated RAW 264.7 macrophage cells. Among the extracts, the EtOAc extract exhibited the most potent NO inhibition, with an IC_{50} value of 6.02 ± 0.65 $\mu\text{g/mL}$, without any cytotoxicity observed, indicating strong anti-inflammatory activity. In comparison, the *n*-butanol extract showed moderate NO suppression, with an IC_{50} value of 15.36 ± 1.47 $\mu\text{g/mL}$, without any cytotoxicity observed. Conversely, the *n*-hexane extract displayed no significant NO suppression activity. These results highlight the EtOAc extract of *D. zibethinus* peels as the most promising candidate for anti-inflammatory applications, followed by the *n*-butanol extract. Given its potent anti-inflammatory and antioxidant activities compared to the other two extracts, the EtOAc extract was selected for further purification and identification of specialized metabolites. Using CC and spectroscopic methods, we aimed to elucidate the structures of the isolated compounds.

3.4. Metabolic profiling of *D. zibethinus* peels

3.4.1. Total phenolic content (TPC)

The TPC of the EtOAc and *n*-butanol extracts was determined using the Folin–Ciocalteu method. The results were 57.70 ± 0.10 mg GAE/g sample of sample for the EtOAc extract and 34.98 ± 0.10 mg GAE/g sample for the *n*-butanol extract.

3.4.2. Volatile compound analysis

To comprehensively identify the components from the fraction that inhibited the HCT116 cell line, GC-MS analysis was conducted using an optimized temperature program and split ratio. The total ion chromatogram is presented in Figure 2. Compounds were identified by comparison to reference spectra from the NIST Mass Spectral Library (NIST 08 Mass Spectral Library, Version 2.0f). As a result, 11 major compounds were identified in Table 3, predominantly

Table 3

Major compounds identified in the *n*-hexane extract of *D. zibethinus* peels through GC/MS analysis.

Peak no.	RT (min)	Compound	Molecular formula	Abundance (%)
1	26.560	<i>n</i> -Hexadecanoic acid	$C_{16}H_{32}O_2$	25.55
2	29.880	Octadecanoic acid	$C_{18}H_{36}O_2$	1.07
3	40.717	Campesteryl acetate	$C_{30}H_{50}O_2$	2.20
4	43.478	Stigmastan-3,5,22-trien	$C_{29}H_{46}$	2.20
5	43.542	Campesterol	$C_{28}H_{48}O$	2.90
6	45.398	6-Methylcholesterol	$C_{28}H_{48}O$	2.04
7	45.844	Stigmasterol	$C_{29}H_{48}O$	5.04
8	46.790	β -Sitosterol	$C_{29}H_{50}O$	41.05
9	47.449	β -Sitosterol acetate	$C_{31}H_{52}O_2$	1.43
10	49.422	9,19-Cyclocholestene-3,7-diol, 4,14-dimethyl-, 3-acetate	$C_{31}H_{52}O_3$	1.96
11	50.198	4,4-Dimethylcholest-5-enol	$C_{29}H_{50}O$	1.25
12	50.280	Stigmastane-3,6-dione	$C_{29}H_{48}O_2$	1.05
		Total identified compounds		86.49%

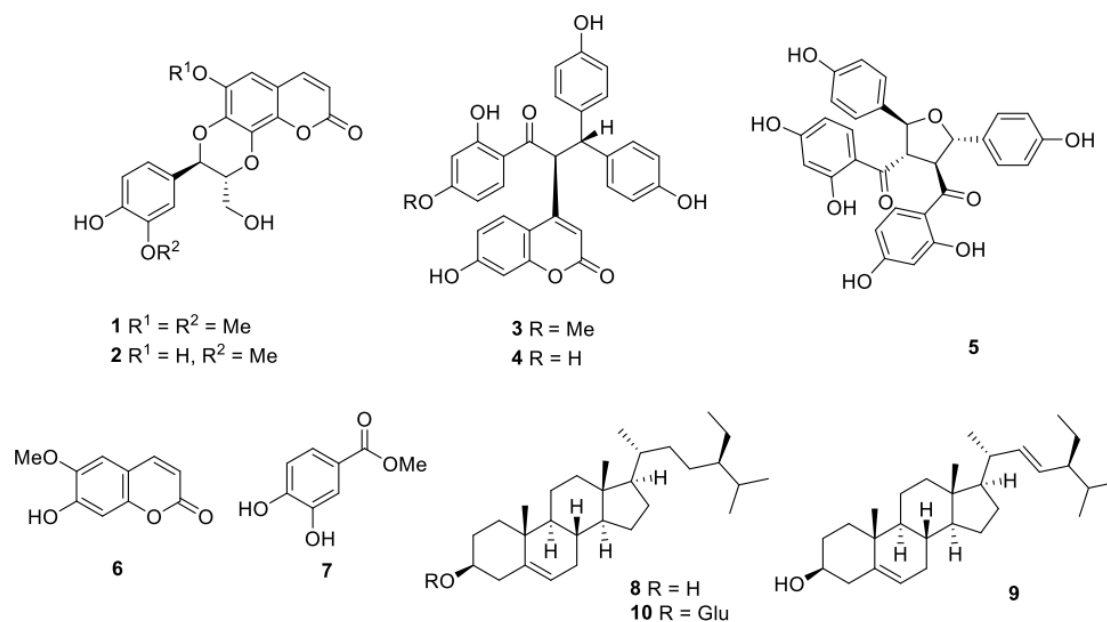


Figure 3. Isolated compounds from the active fractions of *D. zibethinus* peels.

phytosterols, followed by aliphatic derivatives. The total identified compounds accounted for 86.49%.

3.4.3. Isolated compounds of *D. zibethinus* peels

Ten compounds, cleomiscosin A (**1**) (Feng et al., 2016), jatrocinn A (**2**) (Feng et al., 2016), calodenone (**3**) (Messanga et al., 1992), lophirone A (**4**) (Messanga et al., 1992), lophirone G (**5**) (Tih et al., 1990), scopoletin (**6**) (Feng et al., 2016), methyl 3,4-dihydroxybenzoate (**7**) (Rudiyansyah and Garson, 2006), stigmasterol (**8**), β -sitosterol (**9**), and β -sitosterol-*D*-glucoside (**10**) were isolated from the EtOAc extract. Stigmasterol (**8**) and β -sitosterol (**9**) were isolated from the *n*-hexane extract of the peel, yielding the highest quantities among the compounds. Notably, compounds **3**, **4**, and **5** were identified from the *Durio* genus for the first time. The structures of these compounds were elucidated using 1D and 2D NMR spectroscopy, with their identities confirmed by comparison to previously reported data. The structures of the isolated compounds are shown in Figure 3.

3.5. Inhibition of NO production by isolated compounds from *D. zibethinus* peels

Selected compounds (**1–7**) were evaluated for their NO inhibitory activity in LPS-activated RAW 264.7 macrophage cells to assess their anti-inflammatory effects. Compounds **1**, **2**, and **5** demonstrated significant inhibition of NO production, with suppression rates of $78.89 \pm 0.98\%$, $50.52 \pm 4.42\%$, and $66.93 \pm 1.1\%$, respectively. The positive control,

diclofenac, achieved a suppression rate of $54.17 \pm 2.67\%$ at a concentration of $250 \mu\text{M}$. In contrast, compounds **3**, **4**, and **7** exhibited no significant inhibitory activity at the screening concentration of $75 \mu\text{M}$, with suppression levels remaining below 50%.

3.6. Molecular docking

Molecular docking was used to investigate the interaction between compounds **1** and **2** and TLR4/MD2 receptor complex. Molecular docking predicted that compounds **1** and **2** bound with TLR4/MD2 receptor complex, achieving GOLD fitness scores of 55.16 and 55.45, respectively. Hydrogen bonds, hydrophobic interactions, and van der Waal interactions were the main interactions. The amino acids involved with the interactions were shown in Figures 4A and 4B.

3.7. SPF in vitro of crude extracts from *D. zibethinus* peels

The photoprotective capacity of *D. zibethinus* peel extracts was evaluated across three crude extracts, *n*-hexane, EtOAc, and *n*-butanol, and three concentrations as 100, 500, and 1000 ppm, with SPF values measured using a UV-visible spectrophotometer. Results showed a concentration-dependent increase in SPF values across all crude extracts (Figure 4A). For *n*-hexane extract, SPF values ranged from 3.27 to 5.83 at 100–1000 ppm. The EtOAc extract exhibited the highest SPF values, from 4.40 to 16.85, at the same concentration,

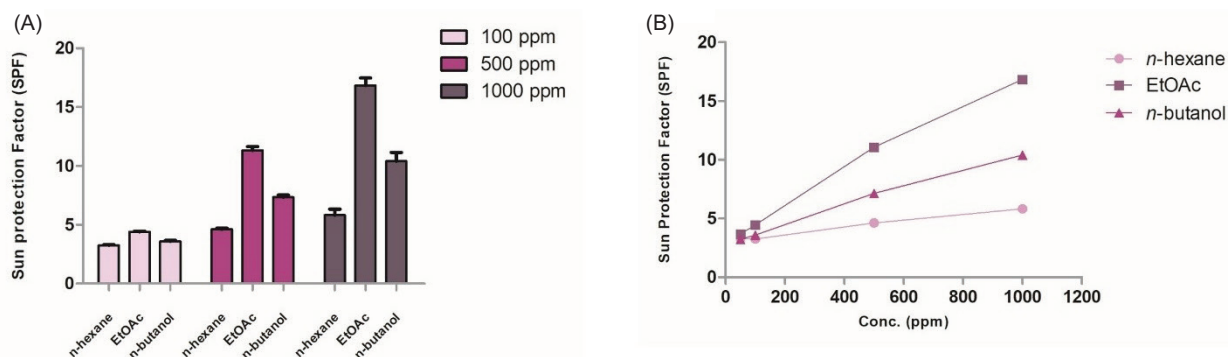


Figure 4. Sun Protection Factor (SPF) of *D. zibethinus* peel extracts (A) and linear plot of in vitro at different concentrations (B).

indicating strong UV-blocking potential in this extract. The *n*-Butanol extract showed intermediate SPF values, from 3.60 to 10.40, at the same concentration. Based on the data, linear equations and coefficients (Figure 4B and Table 4) can be derived for each extract to estimate the concentration needed to achieve a desired SPF value. These equations provide a practical tool for predicting the required amount of each extract for specific photoprotective applications.

4. DISCUSSION

Montong durian (*D. zibethinus*) is often called the “king of fruits” in Thailand because of its distinct flavor, rich nutritional profile, and economic importance (Doraiswamy and Saminathan, 2020; Ho and Bhat, 2015). This durian variety is particularly popular for its creamy texture and sweet taste, and it is highly valued in both local and international markets. Montong durian contains numerous bioactive compounds, including antioxidants like flavonoids, phenolic acids, and carotenoids, contributing to its health benefits (Charoenkiatkul et al., 2016; Zhan et al., 2021). Studies suggest that these compounds possess potential anti-inflammatory, anticancer, and antioxidant properties, making Montong durian more than just a culinary delicacy but also a promising source for functional ingredients in nutraceuticals and cosmetics. Fruits are rich in bioactive compounds, especially phenolic antioxidants, known for their substantial health benefits (Charoenphun and Klangbud, 2022). These molecules help combat oxidative stress by neutralizing free radicals in the body, reducing the risk of chronic diseases like cardiovascular disease, cancer, and neurodegenerative disorders. Besides phenolics, fruits also contain vitamins (such as C and E) and carotenoids, which further contribute to their antioxidant capacity (Doraiswamy and Saminathan, 2020). Regular consumption of fruits, therefore, supports

Table 4

Equations relating the concentration and SPF of *D. zibethinus* peel extracts.

Extract	Linear equation	R^2 value
<i>n</i> -hexane	SPF = 0.0028[Conc.] + 3.1098	0.99
EtOAc	SPF = 0.014[Conc.] + 3.2384	0.99
<i>n</i> -butanol	SPF = 0.0076[Conc.] + 2.9542	0.99

overall health by enhancing the body’s antioxidant defenses and reducing inflammation. Because of the reported bioactive properties of compounds derived from *D. zibethinus*, there is significant interest in their therapeutic potential. The choice of extraction solvent is a crucial determinant in isolating bioactive compounds, particularly phenolic compounds, as it directly impacts the yield, chemical composition, and biological activity of the resulting extracts. In this study, the antioxidant activities of *D. zibethinus* peel extracts were evaluated using solvents with varying polarities, including *n*-hexane, EtOAc, and *n*-butanol, through five radical scavenging assays: DPPH, ABTS, hydroxyl ($\cdot\text{OH}$), superoxide ($\text{O}^{\cdot-}$), and FRAP. The *n*-hexane extract exhibited negligible antioxidant activity, whereas the EtOAc and *n*-butanol extracts demonstrated significant radical scavenging potential across multiple assays. These findings are consistent with previous studies by Charoenphun and Klangbud (Charoenphun and Klangbud, 2022), which reported a strong correlation between TPC and antioxidant activity in durian from Thailand. Phenolic compounds are well-recognized for their ability to donate hydrogen atoms or electrons to neutralize free radicals, thus playing a central role in antioxidant mechanisms. The higher TPC observed in the EtOAc extract corresponds with its superior antioxidant activity, suggesting that phenolic constituents are key contributors to the extract’s bioactivity. Since phenolic compounds are known for their strong radical scavenging

activity, it is reasonable to hypothesize that the extracts exhibiting high antioxidant potential could also reduce inflammatory responses. The anti-inflammatory properties of the three crude extracts from *D. zibethinus* peels were assessed based on their NO suppression activity, quantified through IC₅₀ values. The EtOAc extract demonstrated the most potent NO inhibition among the extracts, highlighting its superior anti-inflammatory potential. The *n*-butanol extract exhibited moderate NO suppression, while the *n*-hexane extract lacked significant activity. These findings position the EtOAc extract as the most promising candidate for anti-inflammatory applications, supported by its combined potent antioxidant and anti-inflammatory activities. Consequently, the EtOAc extract was prioritized for further purification and identification of specialized metabolites, which may provide an insight into the bioactive compounds responsible for its remarkable bioactivity.

From the EtOAc extract, 10 compounds were isolated and identified using a combination of CC and 1D and 2D NMR spectroscopic techniques. The structures of the isolated compounds are depicted in Figure 3. Notably, compounds calodenone (3), lophirone A (4), and lophirone G (5) were identified in the *Durio* genus for the first time. Compounds 1–7 were screened for their NO-suppressive effects, with only compounds 1, 2, and 5 demonstrating the ability to suppress NO production induced by LPS activation. These findings are consistent with previous studies, which have reported that cleomiscosin A (1) and jatrocinn A (2) exhibit anti-inflammatory properties, with IC₅₀ values of 28.88 μM and 21.70 μM, respectively (Feng et al., 2016). The molecular docking analysis supports these observations, as compounds 1 and 2 (corresponding to cleomiscosin A and jatrocinn A, respectively) bound effectively to the TLR4/MD2 receptor complex. These interactions were mediated by hydrophobic interactions, hydrogen bonds, and van der Waals forces with key residues in both the MD2 and TLR4 subunits (Figure 1). Specifically, 1 interacted with Val82, Phe126, Pro127, and Ile153 in the MD2 subunit, while 2 formed interactions with Val82, Phe126, and Pro127, all essential residues for LPS binding (Kawasaki et al., 2003). Additional interactions included Arg90 and Ile124 for D1, and Leu78, Arg90, and Ile124 for D2, which are known targets for small anti-inflammatory agents (Wang et al., 2024). Since LPS induces inflammation by binding to the MD2 subunit, activating inflammatory signaling pathways and increasing the production of pro-inflammatory mediators, such as NO, PGE2, and TNF-α (Ciesielska et al., 2021; Su et al., 2011), the docking results suggest that compounds 1 and 2 could interfere with LPS binding by partially occupying its binding site. This interference potentially reduces inflammation, as reflected in

the observed suppression of NO production. These molecular docking insights strongly support the NO-suppressive activity of the EtOAc extract. The effective interactions of compounds 1 and 2 with the TLR4/MD2 complex reinforce their role as key contributors to the bioactivity of the EtOAc extract, highlighting its potential as a promising candidate for further anti-inflammatory research.

In Hanoi, Vietnam, durian peel extracts have demonstrated cytotoxic activity against MCF7, HepG2, and SK-LU-1 cancer cell lines. However, their cytotoxic potential against HCT116 colorectal cancer cells has not yet been explored. Considering that colorectal cancer is the third most common cancer in Thailand, with a rising incidence in both males and females (Lohsiriwat et al., 2020), investigating effective therapeutic strategies is a critical public health priority. This study specifically focused on evaluating the cytotoxic activity of durian peel extracts against the HCT116 cell line, aiming to bridge the existing knowledge gap and explore their potential as a source of bioactive compounds for the treatment of colorectal cancer. In evaluating the cytotoxic potential of *D. zibethinus* peel extracts against HCT116 colorectal cancer cells using the MTT assay, the *n*-hexane extract demonstrated notable cytotoxicity, significantly surpassing the inhibition rates of the EtOAc and *n*-butanol extracts, which were both below 50% at the same concentration. To comprehensively identify the components responsible for the activity against the HCT116 cell line, GC-MS analysis (Figure 2) identified phytosterols, stigmasterol (8), and β-sitosterol (9) as the major components. These two compounds were also isolated from this extract in this work. They are members of the phytosterol group, a class of plant-derived steroids that exhibit structural and functional similarities to cholesterol. β-Sitosterol is the most prevalent phytosterol, widely distributed across various plant-based foods and commonly found in numerous traditional Thai medicinal herbs. Notably, β-sitosterol has been identified in *Diospyros filipendula* (Wisetsai et al., 2021), *Allophylus cobbe* (Sangsopha et al., 2020), and *Rhodamnia dumetorum* (Lakornwong et al., 2018), among others. β-sitosterol has a wide range of biological functions, including antipyretic, analgesic, antidiabetic, and, most notably, anticancer activities. Extensive research has shown that it exhibits significant antiproliferative effects on various cancer cell lines, including colon cancer cells like HCT116. Studies have highlighted its ability to reduce cell viability and induce apoptosis in these cells, suggesting its role as a chemopreventive and chemotherapeutic agent. Specifically, β-sitosterol interferes with key regulatory pathways that govern cancer cell survival, including those involved in apoptosis and cell cycle regulation. For colon cancer, such as in the HCT116 cell line, β-sitosterol isolated from *Vicia*

monantha has demonstrated potent cytotoxicity against HCT116 colon cancer cells, with an IC_{50} value of 22.61 $\mu\text{g}/\text{mL}$ (El-Halawany et al., 2019). Choi and colleagues further highlighted the apoptotic effects of β -sitosterol on HCT116 cells, noting that at physiologically relevant concentrations, both β -sitosterol and a phytosterol complex significantly reduced cell viability, induced apoptosis, and triggered DNA fragmentation (Choi et al., 2003). These findings suggest that the active fraction, particularly the presence of phytosterols such as β -sitosterol and stigmasterol, may contribute to the observed cytotoxicity against HCT116 cells. Given the correlation between the identified phytosterols and their biological activities, the *n*-hexane extract presents significant potential for further investigation and development as a source of bioactive compounds for cancer therapy.

Plant-derived compounds, mainly phenolic compounds with antioxidant properties and UV-absorbing capacity, have been widely recognized for their potential as natural sunscreen ingredients (Agati et al., 2013; Cavinato et al., 2017). In this study, *D. zibethinus* peel extracts, rich in phenolic content, were evaluated for photoprotective efficacy, demonstrating a concentration-dependent increase in SPF values (Figure 4). The EtOAc extract showed the strongest UV-blocking potential, achieving SPF values of 4.40 to 16.85 across concentrations of 100–1000 ppm, with a linear equation of $\text{SPF} = 0.014[\text{Conc.}] + 3.2384$ ($R^2 = 0.99$) (Table 4). This high slope suggests that the EtOAc extract requires a lower concentration to achieve elevated SPF values compared to *n*-hexane and *n*-butanol extracts. These linear equations provide valuable predictive tools for determining the concentrations needed to achieve targeted SPF levels, with the EtOAc extract standing out as the most promising candidate for further photoprotective applications, such as sunscreen formulations.

5. CONCLUSIONS

Our study demonstrates the bioactive potential of *D. zibethinus* peel extracts across different solvent polarities. The findings underscore the importance of utilizing durian waste for producing health-benefiting products. Future research should focus on optimizing extraction processes such as using greener and safer solvents extraction and conducting *in vivo* studies to validate the therapeutic efficacy and safety of these extracts in humans. The preliminary screening of durian peel extracts for cytotoxicity, antioxidant, and anti-inflammatory properties suggests their possible potential as sustainable, functional ingredients for applications in the pharmaceutical, cosmetic, and food industries, though further studies are needed to confirm these effects..

ACKNOWLEDGEMENT

The authors are thankful for the partial support from the Department of Industrial Chemistry, Faculty of Applied Science, King Mongkut's University of Technology North Bangkok.

AUTHOR CONTRIBUTIONS

Conceptualization, data curation, formal analysis, methodology, project administration, software, visualization, and writing—review and editing were done by A.W.; funding acquisition was done by A.W. and S.J.; investigation was the responsibility of L.T., C.S., A.J., N.S., S.P., and A.W.; resources was the concern of S.J.; validation was looked into L.T., C.S., A.J., and A.W.; writing—original draft was done by L.T., C.S., A.J., S.J., and A.W. All authors have read and agreed to the published version of the manuscript.

CONFLICT OF INTEREST

The authors declare no conflict of interest.

FUNDING

This research budget was allocated by the National Science, Research and Innovation Fund (NSRF), and King Mongkut's University of Technology North Bangkok (Project no. KMUTNB-FF-68-B-34).

ORCID

Awat Wisetsai	0000-0003-4189-5501
Lueacha Tabtimmai	0000-0002-1311-9030
Chanikan Sonklin	0000-0003-0264-5796
Anupong Joompang	0000-0002-9021-5085
Nuttakarn Srisukpachin	0009-0001-8576-6392
Supachai Jadsadajerm	0000-0002-5358-9838
Sutarin Preepram	0009-0002-0028-7753

REFERENCES

- Agati, G., Brunetti, C., Di Ferdinando, M., Ferrini, F., Pollastri, S., Tattini, M. 2013. Functional roles of flavonoids in photoprotection: new evidence, lessons from the past. *Plant Physiology*

- and Biochemistry 72, 35–45. <https://doi.org/10.1016/j.plaphy.2013.03.014>
- Arancibia-Avila, P., Toledo, F., Park, Y.S., Jung, S.T., Kang, S.G., Heo, B.G., Lee, S.H., Sajewicz, M., Kowalska, T., Gorinstein, S. 2008. Antioxidant properties of durian fruit as influenced by ripening. *LWT – Food Science and Technology* 41(10), 2118–2125. <https://doi.org/10.1016/j.lwt.2007.12.001>
- Cavinato, M., Waltenberger, B., Baraldo, G., Grade, C.V.C., Stuppner, H., Jansen-Dürr, P. 2017. Plant extracts and natural compounds used against UVB-induced photoaging. *Biogerontology* 18(4), 499–516. <https://doi.org/10.1007/s10522-017-9715-7>
- Charoenkiatkul, S., Thiyajai, P., Judprasong, K. 2016. Nutrients and bioactive compounds in popular and indigenous durian (*Durio zibethinus* murr.). *Food Chemistry* 193, 181–186. <https://doi.org/10.1016/j.foodchem.2015.02.107>
- Charoenphun, N., Klangbud, W.K. 2022. Antioxidant and anti-inflammatory activities of durian (*Durio zibethinus* Murr.) pulp, seed and peel flour. *Peer J* 10, e12933. <https://doi.org/10.7717/peerj.12933>
- Choi, Y., Kong, K., Kim, Y.A., Jung, K.O., Kil, J.H., Rhee, S.H., Park, K.Y. 2003. Induction of bax and activation of caspases during β -sitosterol-mediated apoptosis in human colon cancer cells. *International Journal of Oncology* 23(6), 1657–1662. <https://doi.org/10.3892/ijo.23.6.1657>
- Ciesielska, A., Matyjek, M., Kwiatkowska, K. 2021. TLR4 and CD14 trafficking and its influence on LPS-induced pro-inflammatory signaling. *Cellular and Molecular Life Sciences* 78(4), 1233–1261. <https://doi.org/10.1007/s00018-020-03656-y>
- Cuong, D.V., Hanh, T.T.H., Huong, N.T., Huong, P.T.M., Vinh, L.B., Quang, T.H. 2023. Secondary metabolites from the fruit peels of *Durio zibethinus* L. and their cytotoxic activity. *Natural Product Research* 37(21), 3556–3562. <https://doi.org/10.1080/14786419.2022.2092733>
- Doraiswamy, R., Saminathan, V. 2020. Phytochemical analysis, antioxidant and anticancer activities of durian (*Durio zibethinus* Murr.) fruit extract. *Journal of Research in Pharmacy* 24(6), 882–892. <https://doi.org/10.35333/JRP.2020.247>
- El-Halawany, A.M., Osman, S.M., Abdallah, H.M. 2019. Cytotoxic constituents from *Vicia monantha* subsp. *monantha* seeds. *Natural Product Research* 33(12), 1783–1786. <https://doi.org/10.1080/14786419.2018.1434638>
- Feng, J., Wang, Y., Yi, X., Yang, W., He, X. 2016. Phenolics from durian exert pronounced NO inhibitory and antioxidant Activities. *Journal of Agricultural and Food Chemistry* 64(21), 4273–4279. <https://doi.org/10.1021/acs.jafc.6b01580>
- Feng, J., Yi, X., Huang, W., Wang, Y., He, X. 2018. Novel triterpenoids and glycosides from durian exert pronounced anti-inflammatory activities. *Food Chemistry* 241, 215–221. <https://doi.org/10.1016/j.foodchem.2017.08.097>
- He, Y., Peng, L., Xiong, H., Liu, W., Zhang, H., Peng, X., Zhu, X., Guo, F., Sun Y. 2023. The profiles of durian (*Durio zibethinus* Murr.) shell phenolics and their antioxidant effects on H₂O₂-treated HepG2 cells as well as the metabolites and organ distribution in rats. *Food Research International* 163, 112122. <https://doi.org/10.1016/j.foodres.2022.112122>
- Ho, L.H., Bhat, R. 2015. Exploring the potential nutraceutical values of durian (*Durio zibethinus* L.) – An exotic tropical fruit. *Food Chemistry* 168, 80–89. <https://doi.org/10.1016/j.foodchem.2014.07.020>
- Karamać, M., Kosińska-Cagnazzo, A., Kulczyk, A. 2016. Use of different proteases to obtain flaxseed protein hydrolysates with antioxidant activity *International Journal of Molecular Sciences* 17(7), 1027. <https://doi.org/10.3390/ijms17071027>
- Kawasaki, K., Nogawa, H., Nishijima, M. 2003. Identification of mouse MD-2 residues important for forming the cell surface TLR4-MD-2 complex recognized by anti-TLR4-MD-2 antibodies, and for conferring LPS and taxol responsiveness on mouse TLR4 by alanine-scanning mutagenesis. *The Journal of Immunology* 170(1), 413–420. <https://doi.org/10.4049/jimmunol.170.1.413>
- Kongkachuichai, R., Charoensiri, R., Sungpuag, P. 2010. Carotenoid, flavonoid profiles and dietary fiber contents of fruits commonly consumed in Thailand. *International Journal of Food Sciences and Nutrition* 61(5), 536–548. <https://doi.org/10.3109/09637481003677308>
- Lakornwong, W., Kanokmedhakul, K., Kanokmedhakul, S. 2018. A new coruleoellagic acid derivative from stems of *Rhodamnia dumetorum*. *Natural Product Research*. 32(14), 1653–1659. <https://doi.org/10.1080/14786419.2017.1395430>
- Lohsiriwat, V., Chaisomboon, N., Pattana-Arun, J. 2020. Current colorectal cancer in Thailand. *Annals of Coloproctology* 36(2), 78–82. <https://doi.org/10.3393/ac.2020.01.07>
- Messanga, B.B., Tih, R.G., Kimbu, S.F., Sondengam, B.L., Martin, M.T., Bodo, B. 1992. Calodenone, a new isobiflavonoid from *Ochna calodendron*. *Journal of Natural Products* 55(2), 245–248. <https://doi.org/10.1021/np50080a018>
- Mota, A.H., Andrade, J.M., Rodrigues, M.J., Custódio, L., Bronze, M.R., Duarte, N., Baby, A., Rocha, J., Gaspar, M.M., Simões, S., Carvalheiro, M., Fattal, E., Almeida, A.J., Reis, C.P. 2020. Synchronous insight of in vitro and in vivo biological activities of *Sambucus nigra* L. extracts for industrial uses. *Industrial Crops and Products* 154, 112709. <https://doi.org/10.1016/j.indcrop.2020.112709>
- Nerys, L.L., Jacob, I.T.T., Silva, A.R., Oliveira, A.M., Rocha, W.R.V., Pereira, D.T.M., Abreu, A.S., Silva, R.M.F., Filho, I.J.C., Lima, M.D.C.A. 2022. Photoprotective, biological activities and chemical composition of the non-toxic hydroalcoholic extract of *Clarisia racemosa* with cosmetic and pharmaceutical applications. *Industrial Crops and Products* 180, 114762. <https://doi.org/10.1016/j.indcrop.2022.114762>
- Numee, P., Sangtawesin, T., Yilmaz, M., Kanjana, K. 2024. Activated carbon derived from radiation-processed durian shell for energy storage application. *Carbon Resources Conversion* 7(2), 100192. <https://doi.org/10.1016/j.crcon.2023.07.001>
- Payus, C.M., Refdin, M.A., Zahari, N.Z., Rimba, A.B., Geetha, M., Saroj, C., Gasparatos, A., Fukushi, K., Alvin Oliver, P. 2021. Durian husk wastes as low-cost adsorbent for physical pollutants removal: groundwater supply. *Materials Today: Proceedings* 42, 80–87. <https://doi.org/10.1016/j.matpr.2020.10.006>
- Phoengmak, W., Sirivongpaisal, N., Sridach, W., Naemsai, T., Thongkaew, K. 2023. Effects of the precooling process on the preservation of fresh-cut durian. *Journal of Food Process Engineering* 46(12), e14463. <https://doi.org/10.1111/jfpe.14463>
- Pimsamarn, J., Kaewtrakulchai, N., Wisetsai, A., Mualchonham, J., Muidang, N., Jiraphothikul, P., Autthanit, C., Eiad-Ua, A., Laosiripojana, N., Jadsadajerm, S. 2024. Torrefaction of durian peel in air and N₂ atmospheres: impact on chemical properties and optimization of energy yield using multilevel factorial design *Results in Engineering*. 23, 102767. <https://doi.org/10.1016/j.rineng.2024.102767>

- Rudiyansyah Garson, M.J. 2006. Secondary metabolites from the wood bark of *Durio z ibethinus* and *Durio k utejensis*. Journal of Natural Products 69(8), 1218–1221. <https://doi.org/10.1021/np050553t>
- Sah, B.P., Pathak, T., Sankar, S., Suresh, B. Phytochemical investigations on the fruits of *Durio zibenthinus* Linn. For Antimicrobial Activity. International Journal of Pharma Sciences and Research 5(12), 878–891.
- Sangsopha, W., Schevenels, F.T., Lekphrom, R., Kanokmedhakul, S. 2020. A new tocotrienol from the roots and branches of *Allophylus cobbe* (L.) Raeusch (Sapindaceae). Natural Product Research 34(7), 988–994. <https://doi.org/10.1080/14786419.2018.1547298>
- Sonklin, C., Alashi, A.M., Laohakunjit, N., Aluko, R.E. 2021. Functional characterization of mung bean meal protein-derived antioxidant peptides. Molecules 26(6), 1515. <https://doi.org/10.3390/molecules26061515>
- Su, Y.W., Chiou, W.F., Chao, S.H., Lee, M.H., Chen, C.C., Tsai, Y.C. 2011. Ligustilide prevents LPS-induced iNOS expression in RAW 264.7 macrophages by preventing ROS production and down-regulating the MAPK, NF- κ B and AP-1 signaling pathways. International Immunopharmacology 11(9), 1166–1172. <https://doi.org/10.1016/j.intimp.2011.03.014>
- Tabtimmai, L., Jongruksavongkul, C., Wisetsai, A., Sonklin, C., Aiamsung, M., Chamsodsai, P., Choowongkamon, K., Sedtananon, S. 2024. Three-phase partitioning technique for the green separation of crude polysaccharides from *Schizophyllum commune* and its effect on macrophage activation. Food Bioscience 58, 103735. <https://doi.org/10.1016/j.fbio.2024.103735>
- Tan, X.Y., Misran, A., Daim, L.D.J., Ding, P., Pak Dek, M.S. 2020. Effect of freezing on minimally processed durian for long term storage. Scientia Horticulturae 264, 109170. <https://doi.org/10.1016/j.scienta.2019.109170>
- Tih, R.G., Sondengam, B.L., Martin, M.T., Bodo, B. 1990. Structure of the chalcone dimers lophirone F, and H from *Lophira lanceolata* stem bark. Phytochemistry 29(7), 2289–2293. [https://doi.org/10.1016/0031-9422\(90\)83054-5](https://doi.org/10.1016/0031-9422(90)83054-5)
- Wang, J., Zhou, Y., Zhang, J., Tong, Y., Abbas, Z., Zhao, X., Li, Z., Zhang, H., Chen, S., Si, D., Zhang, R., Wei, X. 2024. Peptide TaY attenuates inflammatory responses by interacting with myeloid differentiation 2 and inhibiting NF- κ B signaling pathway. Molecules 29(20), 4843. <https://doi.org/10.3390/molecules29204843>
- Wisetsai, A., Schevenels, F.T., Lekphrom, R. 2021. Chemical constituents and their biological activities from the roots of *diospyros filipendula*. Natural Product Research 35(16), 2739–2743. <https://doi.org/10.1080/14786419.2019.1656630>
- Zhan, Y., Hou, X., Fan, L., Du, Z., Ch'ng, S.E., Ng, S.M., Thepkaysone, K., Hao, E., Deng, J. 2021. Chemical constituents and pharmacological effects of durian shells in ASEAN countries: a review. Chinese Herbal Medicine 13(4), 461–471. <https://doi.org/10.1016/j.chmed.2021.10.001>